Single Acquisition Electrical Property Mapping

José P. Marques[1], Daniel K. Sodickson[2], Christopher M. Collins[2], and Rolf Gruetter[3,4]

[1]*CIBM, University of Lausanne, Lausanne, Vaud, Switzerland,* [2]*Bernard and Irene Schwartz Center for Biomedical Imaging, Department of Radiology, New York University School of Medicine, New York, NY, United States,* [3]*LIFMET - Laboratory for Functional and Metabolic Imaging, EPFL, Lausanne, Vaud, Switzerland,* [4]*Department of Radiology, Universities of Geneva and Lausanne, Lausanne, VD, Switzerland*

Introduction : Electrical property mapping has been a subject of increasing interest in recent years. Noninvasive maps of electric conductivity (σ) and permittivity (ε) *in vivo* could find applications in various fields, including SAR control in high field MRI, design of subject specific head models for TMS, EEG and MEG, and direct medical diagnostics. All methods to map conductivity together with permittivity presented to date rely on multiple acquisitions in order to compute quantitative magnitude RF transmit fields, B_1^+, and either: (a) make assumptions regarding the phase of the RF field that may not be valid at high field strength [1,2,3]; (b) use multiple transmit coils to estimate the absolute RF phase [4]; or compute absolute RF phase by combining B_1^+ maps with receive B_1^- maps [5]. In this work we propose a formalism to compute electrical property maps based solely on relative receive coil sensitivities and demonstrate the feasibility of this approach in simulations and phantom data.

Methods: The Helmholtz equation $\frac{\nabla^2 B_1^{\pm}}{B_1^{\pm}} = -(\mu\varepsilon\omega^2 \pm i\mu\sigma\omega)$ [Eq. 1] is valid in regions of constant σ and ε. Although absolute B_1^- fields cannot be measured, relative receive field between two coils, $B'^-_{1,i,ref}$, can be measured from any MR acquisition as $B'^-_{1,i,ref} = \frac{Signal_i}{Signal_{ref}} = \frac{B^-_{1,i}}{B^-_{1,ref}}$, where $Signal_i$ is the signal measured by coil *i*. Given that the conductivity and permittivity experienced by any of the receive coils is the same, $\left(\frac{\nabla^2 B^-_{1,i}}{B^-_{1,i}} = \frac{\nabla^2 B^-_{1,ref}}{B^-_{1,ref}}\right)$, it is possible to build a set of linear equations $-2\nabla B'^-_{1,i,ref} \cdot \frac{\nabla B^-_{1,ref}}{B^-_{1,ref}} = \nabla^2 B'^-_{1,i,ref}$ [Eq. 2] which can be solved for the gradients of the unknown absolute reference field, $\nabla B^-_{1,ref}/B^-_{1,ref}$, if four or more receive coils are available. Electrical properties can subsequently be computed by rewriting the Helmholtz equation as a function of $\nabla B^-_{1,ref}/B^-_{1,ref}$: $\frac{\nabla^2 B^-_{1,ref}}{B^-_{1,ref}} = \frac{\nabla B^-_{1,ref}}{B^-_{1,ref}} \cdot \frac{\nabla B^-_{1,ref}}{B^-_{1,ref}} + \nabla \cdot \left(\frac{\nabla B^-_{1,ref}}{B^-_{1,ref}}\right) = -(\mu\varepsilon\omega^2 - i\mu\sigma\omega)$ [Eq. 3]

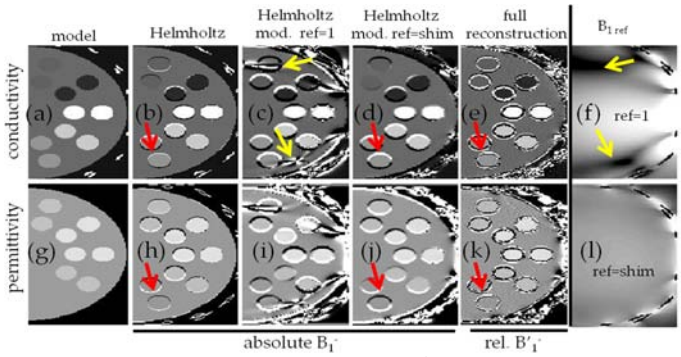

Figure 1 conductivity and permittivity maps of a transverse slice across the numerical phantom are shown in the top and bottom rows respectively. The columns show: (a,g) - modeled maps, (b,h) - maps reconstructed when using Eq.1 assuming B_1^- of all coils is fully known; (c,i) and (d,j) - maps reconstructed using modified Helmholtz equation (Eq.4) with either one single coil (f) or a locally shimmed set of phase-matched coil combinations (l) assuming B_1^- of all coils is fully known; (e,k) reconstructed maps starting from relative receive coil sensitivities and using as the reference the principal mode in the sliding window kernel. Red arrows highlight the artifacts present in tissue interfaces where the conductivity or permittivity are not constant. Yellow arrows highlight the sensitivity of the modified Helmholtz equation to numerical errors arising from a low B_{1ref}^-, which can be overcome by choosing a suitable mode in the kernel.

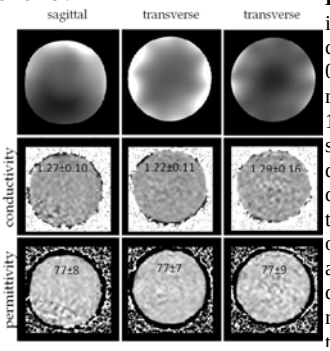

Figure 2 Magnitude ima-ges (top), conductivity (middle 0-2S/m) and per-mittivity (bottom 1-100) maps across the sagittal and transverse directions (in two different acquisi-tions).Values overlaid on the maps are average and standard deviation in large region of interest in the displayed slice.

Numerical Simulations (NS): A transceive array with 16 loop elements surrounding a spherical (d=160mm) phantom (σ=0.75 and ε=65) including smaller spheres with varying conductivity (0.2-2.1) and permittivity (40-90) was simulated at 300MHz using XFDTD v6.4 (Remcom, Inc.).

Phamtom Data (PD): A 3DGRE multi echo sequence was used, with parameters TR/TE1/TE2= 15/3.5/9.92ms, α =1/15 degree, res=1mm isotropic, Matrix size 192x192x192 T_{acq}=10min. A spherical water phantom (160mm diameter filled with 8.2g $NaC_2H_3O_2$ and 9.6g $C_3H_3O_3Li$ per 1000g H_2O) was scanned on a 7T MR scanner (Siemens Medical Solutions, Erlangen, Germany) using a 32-element receive array (Nova Medical Inc).

Electrical property map reconstruction: ***(i)*** calculations were performed in a sliding window of width $L+2K_{Grad}$(L_{NS}=4 ; L_{PD}=15); ***(ii)*** Coil modes were computed via SVD decomposition in the center L^3 kernel, and 5 relative $B_{1,i,ref}^-$' were computed using the first mode as reference (Eq.2); ***(iii)*** Gradients were calculated using either finite differences (K_{GradNS}=2), or a gaussian smoothed gradient kernel (K_{GradNS}=7); ***(iv)*** Eq.2 was solved by Moore-Penrose matrix inversion for each pixel; ***(v)*** Eq.3 was computed and the electrical properties calculated in the inner kernel of width L.

Results - Figure 1 shows the results of the NS, where a high correlation (0.99) was found between the calculated and modeled properties when the boundaries (where Eq.1 is not valid) are neglected. Figure 2 shows reconstructed phantom properties obtained with two different parameter sets showing robustness to effects such as incomplete rf spoiling and echo time. The conductivity values are in good agreement with known values for the sodium concentration of 0.89% [3].

Discussion - Electrical property mapping based on relative receive sensitivity maps has been demonstrated in simulations and experimentally on phantom data. Although the method suffers from increased sensitivity to noise and derivative estimation error compared to published methods [4,5] (because it relies on third order derivatives), this is offset by the fact that relative receive fields can be measured with the most SNR efficient sequences. The main advantages of the methodology are: (a) it is based on a single measurement (which is faster and less prone to subject motion than multiple-measurement approaches); (b) it does not rely on the measurement of B_1^+ maps (whose accuracy and precision is limited)[1-5], or on specific coil/subject setups [1-4]; (c) it is insensitive to practical complications such as frequency inhomogeneities or eddy currents [3]. Future work will be directed towards denoising the relative receive maps and their derivatives so that high-resolution electrical properties can be meaningfully applied *in vivo* where tissue boundaries may lie only a few millimeters from each other.

References[1] Katscher et al. IEEE, **28**, 2009; [2] Voigt et al, MRM, **66**, 2011; [3] van Lier et al, MRM, 67, 2012; [4] Katscher et al, MRM, 2012; [5] Sodickson et al, ISMRM, 2012,387